

TO DIRECTLY DRIVEN AND LOADING-UNLOADING PROCESSES DURING SUBSTORM

Y. I. Feldstein, L. I. Gromova, A. E. Lcvitin

IZMIRAN, 142092 Troitsk, Moscow Region, Russia
phone: 7-095-334-0286; e-mail: gromova@izmiran.rssi.ru

L.G.Blomberg, G.T.Marklund, and P.-A. Lindqvist

Alfven Lab., Royal Inst.Technol., S-100 44 Stockholm, Sweden
phone: 46-8-790-7695; e-mail: makrlund@plasma.kth.se

ABSTRACT

Model calculations of the electric fields in the high-latitude ionosphere are compared to measurements made by the Viking satellite during August 3, 1986 pass. The model calculations are based on the IZMEM procedure, where the electric field and currents in the ionosphere are given as functions of the interplanetary magnetic field (IMF). The event chosen correspond to the growth phase of substorm. The correlation between the model results and the satellite data is high, which assumes directly driven of the magnetosphere by the solar wind. Similar high correlation exists between the electric field in the solar wind ($V \cdot B_s$) and AL magnetic activity indices, if time delays between the $V \cdot B_s$ observations in space and magnetic activity above the Earth's ground are taken into account. It is concluded, that the directly driven response of the magnetosphere to highly variable solar wind electric field is the main feature of geomagnetic activity at high latitudes.

1. INTRODUCTION

Akasofu (Ref. 1 & Ref. 2) drew attention to the existence in the magnetosphere of two energy dissipation mechanisms, namely, "directly driven" by the solar wind and due to an "unloading processes" in the magnetospheric tail. For the driven activity it was suggested that close correlation exists among geoeffective characteristics of the solar wind (in particular, the interplanetary magnetic field IMF) and geomagnetic activity (Ref.3). In a simply driven system the response show some time delay, but would reflect of the major variability of the solar wind velocity and IMF fluctuations. Unloading process is connected with dissipation of energy preliminary stored in the magnetospheric tail (Ref. 4). As an inner magnetospheric process it is less closely tied with the solar wind parameters. For an unloading process, one would in general expect quite different time dependencies for solar wind energy input and the resultant magnetospheric response. The magnetosphere could store energy for long periods of time (hours) and then could dissipate the energy on time scales very different from those characteristic of the loading time. Apparently, both processes occur during magnetic

substorms intervals. However, their relative contribution to the magnetospheric activity can vary in the course of a substorm (Ref. 5). Below, for determination of character of interaction between the solar wind and magnetosphere, comparison was conducted of electric fields obtained on the basis of model calculations and measured by Viking satellite. IZMEM (IZMiran Electrodynamic Model) model was used for calculations, it allows for any set of parameters of the solar wind to define model values of the electrostatic potential, electric field, ionospheric and field-aligned currents (Ref. 6 & Ref. 7). Usage of the model makes it possible to divide spatial and temporal variations of the electric field and obtain in pure form the electric field temporal variations by satellite observations. It is supposed, that good correlation between model and observed electric fields means direct influence of the interplanetary environment on the electromagnetic condition inside magnetosphere (the directly driving mechanism) as linear connection between the electric field in the magnetosphere and the IMF is put to the model calculations. Section 2 contains comparison between measured and model electric fields for Viking pass on August 3, 1986 during the growth phase of magnetospheric substorm. Re-examination of driven and unloading aspects of magnetospheric substorms is presented in section 3. The last section contains a discussion of the results and conclusions of this study.

2. CONVECTION AND ELECTRIC FIELD VARIATIONS OVER THE IONOSPHERE DURING THE GROWTH PHASE OF MAGNETOSPHERIC SUBSTORM

Let us consider, as an example, results of comparison of model and observed electric field measurements along Viking orbit 896 at high latitudes of northern hemisphere on August 3, 1986 (17.10UT - 19.20UT). Fig.1 presents average 1 min values of E2 component of electric field (transversal to magnetic field and directed nearly opposite to the satellite's velocity vector), the IMF B_z and B_y components variations and auroral electrojets indices AU, AL and AE (Ref. 8). At 18UT AU and AL indices begin to increase, which means the smooth increase of both the eastward and

westward electrojets. The magnetic field variations along the EISCAT chain of magnetic observatories in the near midnight sector showed that the substorm expansion phase onset occurred at 20.15UT. Before this moment the decrease of the X-component of geomagnetic field has maximum at geomagnetic latitudes in the $70^\circ < \Phi < 72^\circ$ range with practical absence of disturbances in $\Phi \sim 67^\circ$. Such character of the geomagnetic field variations is typical for the growth (creation) phase of a magnetospheric substorm (Ref. 9 & Ref. 10). Thus, Viking pass began during relatively quiet magnetospheric conditions and finished during the substorm growth (creation) phase.

Substantial changes of the IMF components occur (Fig. 1) in the course of interval of Viking intersection of high-latitude region (about 2 hours). Therefore the model electric fields substantially changes during the satellite pass and for their calculations temporal variations of the IMF ought to be taken into account. Such time-dependence was taken into account in the model calculations of the electric field along the Viking pass presented in Fig. 2a,b. The E^m distribution was calculated every 5 min for entire high-latitude region and for each point along the satellite pass, the electric field vector representative of that location and time is plotted in Fig. 2a. A time delay of 10 min was assumed between the IMF and the electric field response.

Viking measured the horizontal electric field in a direction approximately antiparallel to the satellite velocity vector. Fig. 2b presents the variations of the model electric field $E2^m$ projected onto the same direction as the electric field measurements on board the satellite. Negative values correspond to electric field pointing roughly in the satellite direction of motion (Ref. 11).

$E2^m$ values were calculated for mean the IMF component values with a time step from 1 min to 15 min and the delay time of $E2^m$ relative to the IMF changed from 10 min to 25 min. When correlating E2

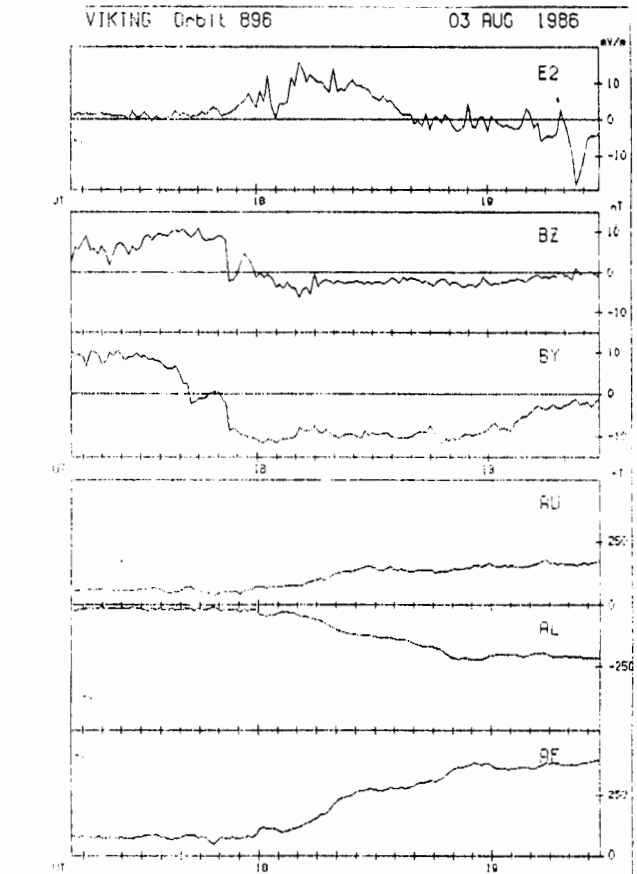
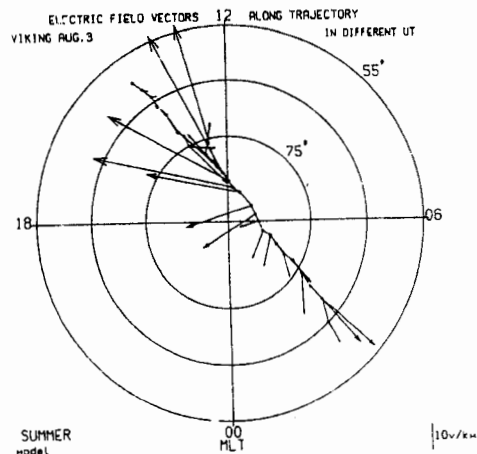


Figure 1. One minute mean values during 896 pass of Viking via the high-latitude region of the following parameters are presented: the transversal component of electric field $E2$ recorded by Viking satellite; Bz and By IMF components measured by IMP-8 spacecraft (its position is $X = 32.4R_e, Y = -16.8R_e, Z = -12.4R_e$); AU, AL and AE indices of magnetic activity.

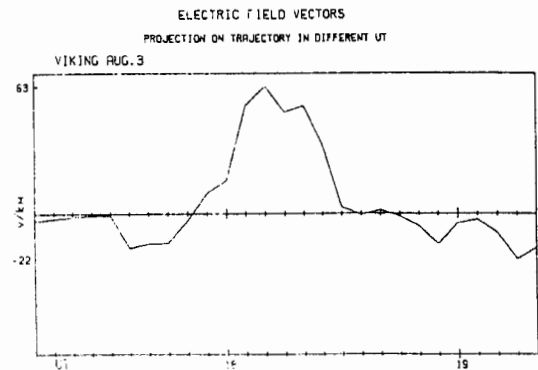


Figure 2. Distribution of the high-latitude electric field vectors on August 3, 1986 for every 5 min of UT along the Viking pass. The temporal variations of the IMF By and Bz components have been accounted for when calculating the electric field as a 10 min time delay between the IMF and the ionospheric response. Model electric field vectors plotted along the Viking trajectory every 5 min (a). Projection of the electric field vectors to the direction of axis 2 in the spin plane (b).

and $E2^m$, a change of the electric field magnitude with altitude need to be taken into account. As $E2^m$ corresponds to the ionosphere dynamo-region height where ionospheric current flow, the $E2$ values were mapped from the satellite altitude (8,000 - 13,000 km) to 100 km height using the assumption of no parallel potential drop between the two altitudes.

Fig. 3 presents $E2^m$ and $E2$ variations for different time steps from 1 min to 5 min with the IMF delay time $\Delta T = 20$ min. The correlation coefficient (RR) and the mean square deviation (dispersion DISP) between $E2^m$ and $E2$ along Viking pass were calculated for every time step. It follows from Fig. 3 that reasonably good agreement exists between the modelled and observed electric fields. Values of RR and DISP for 10 min and 15 min time steps are at the same level as for 5 min time step.

Fig. 4 presents $E2^m$ and $E2$ variations for different

values of IMF delay time ΔT with time step in 5 min. The improvement of correlation up to $RR = 0.9$ with ΔT increases from 10 min to 20 min takes place. Then the value of RR decreases as ΔT increases.

The high correlation between observed and modelled electric field values above the ionosphere indicates to the close control of the magnetosphere electromagnetic condition by the IMF during a substorm growth (creation) phase. Apparently, the magnetosphere at this phase of substorm is a system directly driven by the solar wind. Intramagnetospheric processes connected with the unloading of magnetic energy stored in the magnetospheric tail have only auxiliary role.

3. RE-EXAMINATION OF DRIVEN AND UNLOADING ASPECTS OF MAGNETOSPHERE SUBSTORMS

According to Baker (Ref. 12) for isolated substorms the magnetosphere-ionosphere system exhibits a bimodal response to solar wind changes. A 20-min

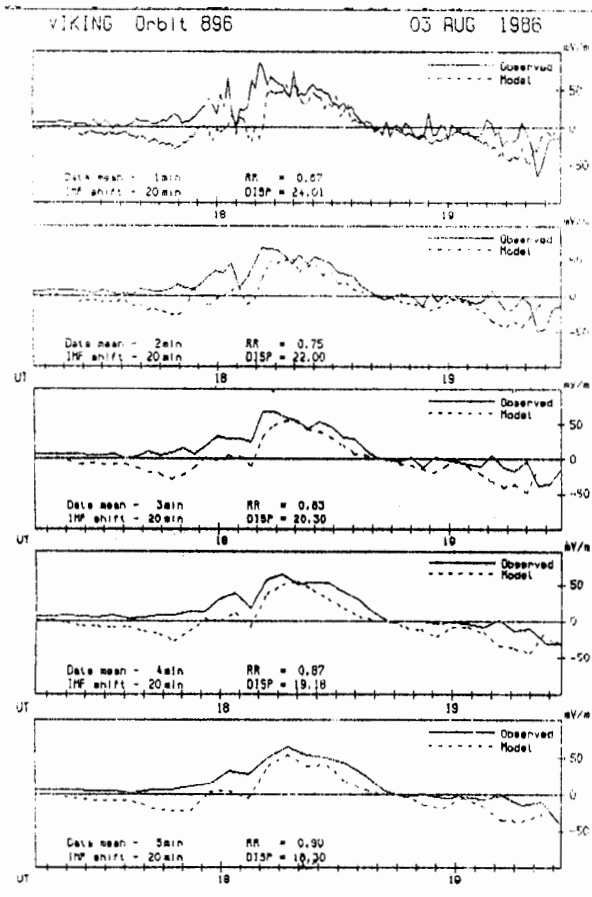


Figure 3. Comparison of the horizontal electric field components measured by Viking satellite and mapped along the dipole magnetic field-line on the 100 km altitude ($E2$ solid line) and calculated ($E2^m$ dotted line) with various averaging time step for the IMF and $E2$ values but with the constant the IMF time shift $\Delta T = 20$ min. From top to the bottom time step values of 1 min, 2 min, 3 min, 4 min and 5 min are presented. The correlation coefficient and mean square deviations values are presented as well.

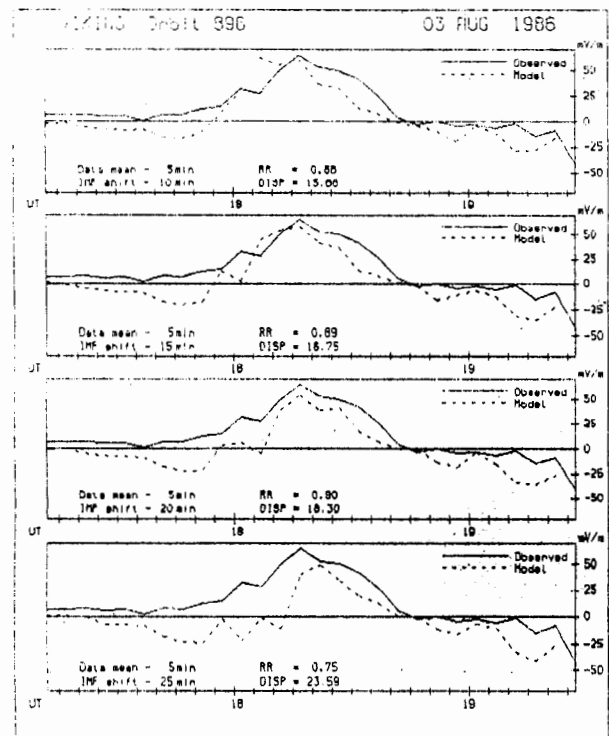


Figure 4. Comparison of $E2$ and $E2^m$ for various values of the IMF time shifts ΔT relative to $E2$ with the constant value of time step equals 5 min.

response characteristic is associated with the driven aspect of substorm, while a 1-hr response time is associated with unloading. Akasofu (Ref. 13) has announced that the main role of the directly driven process between a solar wind and magnetosphere in occurrence of magnetospheric substorm became conventional. Thus he refers to such strong proponent

of the loading-unloading process as D. Baker (Ref. 14). In Ref. 14 interrelationship between the solar wind electric field ($V \cdot B_s$) and the AL geomagnetic activity index at 2.5 min resolution was investigated based on big data array. It appeared "that realistic replications of the AL index result from the non-linear model simulations if unloading is permitted in the model. If unloading is not included, i.e. if only a driven response is permitted, then the resulting simulation of AL is unrealistic in its amplitude and temporal evolution". This conclusion was substantiated by comparison of $V \cdot B_s$ with AL for 30 time intervals during 1973-74. These intervals of complete continuous solar wind coverage were typically several days long, they were merged together as a single time series with total duration of 1,800 hours.

Temporal shift between $V \cdot B_z$ and AL for receipt the maximum possible correlation can change from event to event. Therefore, merging to single time array long series of measurements inevitably leads to conservative value of correlation coefficient when comparing such series. For revelation of the directly driven component long intervals with continuous the IMF and solar plasma measurements by IMP-8 satellite were selected in AL indices of magnetic activity. During 1986 year 91 of such intervals were chosen with the length between 7 and 22 hours. 20,427 mean 5-min values of AL and $V \cdot B_z$ were received (about 1,700 hours). Fig. 5 shows changes of 5-min values of $V \cdot B_s$ and AL, where B_s is the IMF southward component. The value of correlation coefficient between the two series with zero time shift is only 0.32. Low correlation between AL and $V \cdot B_s$ may be interpreted as insignificant contribution of directly driven process to the magnetic disturbances generation. In this case the obtained result agrees with conclusions of Baker et al. (Ref. 14).

As was discussed in the previous section, the magnitude of correlation coefficient between the solar wind geoeffective parameters and their geophysical response depends substantially on the time shift between these two series. Therefore we calculated correlation coefficients between $V \cdot B_z$ and AL for all 91 intervals with time shift changing from 0 min to 120 min. For 5-min intervals with $B_z > 0$ value of $V \cdot B_z$ is set equal to zero. Fig. 6 presents, as an example,

characteristical variations of correlation coefficient RR for three time intervals. It is clear, that the coefficient magnitude depends substantially on time shift ΔT value. There are cases, when for $\Delta T = 0$ correlation is practically absent, but RR exceeds 0.5 for $\Delta T = 1$ hour. Values of ΔT , when RR reaches maximum value, vary from one interval to another. It means that when correlating $V \cdot B_z$ and AL big data arrays should not be used as they are compiled from intervals with different time shift. As a result, usage of big arrays

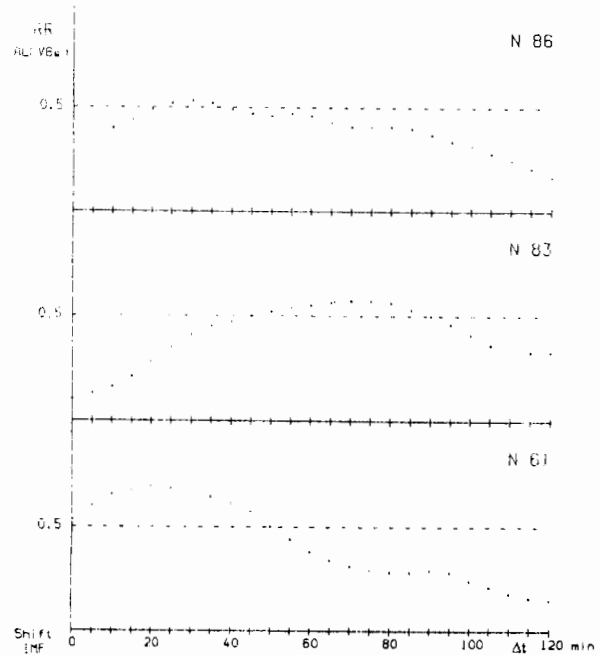


Figure 6. The variations of RR ($V \cdot B_z$, AL) in dependance on time shift ΔT between $V \cdot B_z$ and AL. Clearly expressed changes of RR exist and they vary for different time interval.

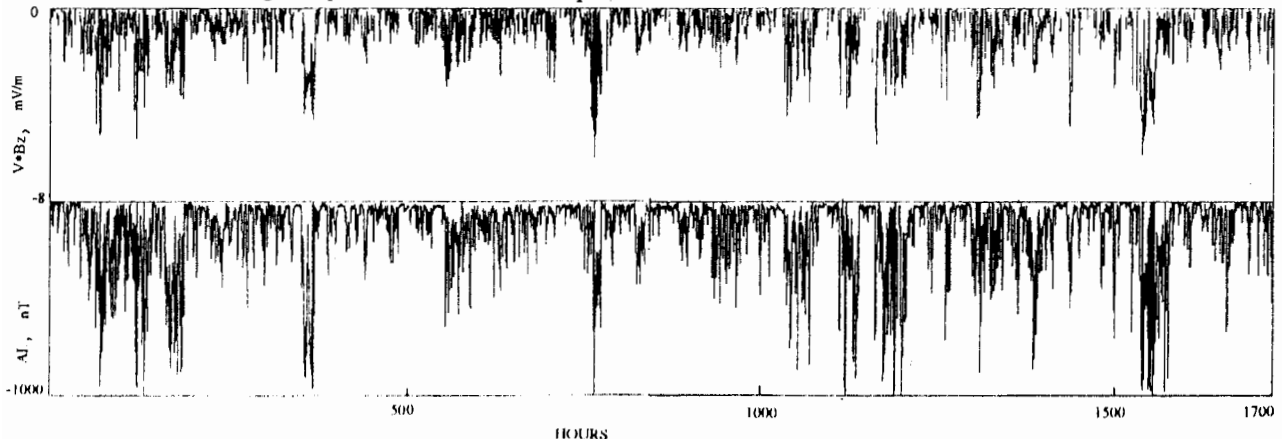


Figure 5. The composite data set of $V \cdot B_s$ (top) and AL (bottom) at 5 min resolution; compiled from 91 time intervals in 1986 (all in all 20,427 values). The correlation coefficient between AL and $V \cdot B_s$ using all available data with zero time shift is 0.32.

underestimates the contribution of directly driven process.

Fig. 7 shows distribution of amount of cases with maximum RR values for intervals with no less than 100 cases with 5 min intervals of the southward IMF. For absolute majority of these cases correlation is notable ($0.4 \leq RR \leq 0.8$), which means existence of substantial direct influence of the solar wind on magnetic disturbance in the auroral zone. Equations of linear regression were determined for time shifts leading to maximum correlation between AL and $V \cdot B_z$. It allows to compare quantitatively observed and modeled AL values. Fig. 8 presents results of such comparison for interval N°61 on September 25-26, 1986. In this concrete event the equation has the following form: $AL = 0.2 \cdot V \cdot B_z - 214$, where AL is in nT, $V \cdot B_z$ is in $\text{km} \cdot \text{nT} / \text{sec}$. It is clear, that the AL component directly connected with the solar wind geoeffective parameter $V \cdot B_z$ is a considerable part of observed on the Earth's ground magnetic disturbances in the auroral zone.

4. DISCUSSION AND SUMMARY

To summarize the results, we have demonstrated that the electric field in the magnetosphere during growth phase of the magnetospheric substorm is closely connected with the solar wind geoeffective parameters. In other words, the directly driven mechanism of the solar wind interaction with the Earth's magnetosphere is realized. According to Ref. 5, this mechanism determines the electric field variations in the magnetosphere not only at the growth phase, but at the substorm expansion phase as well. Usage of AL indices of geomagnetic activity for revelation of directly driven process does not pinpoint as close relationship of magnetic activity at auroral latitudes with the solar wind electric field, as it was the case when using measurements of electric field in the ionosphere. This result may be the consequence of two causes:

- i) the electric field in the magnetosphere is better indicator for revealing existence of the directly driven mechanism, than indices of the magnetic activity. The intensity of AL is determined not only by the electric field magnitude in the magnetosphere, but is largely defined by integral conductivity of the ionosphere which depends on corpuscular precipitation from the plasma sheet of the magnetospheric tail. Consequently the contribution of directly driven process to generation of magnetic disturbances is underestimated. The observations of the electric field appear more suitable for revealing of process responsible for the nature of interaction between the solar wind and the magnetosphere, than geomagnetic activity indices;
- ii) usage for revelation of relationship between $V \cdot B_z$ and AL dependence of the correlation coefficient magnitude from time shift ΔT between the solar wind processes and their response in the Earth's magnetosphere. Value of ΔT varies from one event to another and merging of many disturbed intervals to a single array leads, as a result, to substantial decrease of

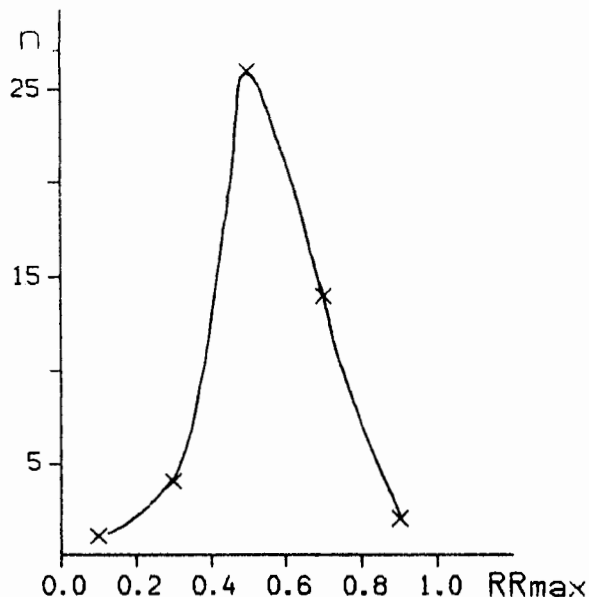


Figure 7. Distribution of amount of cases with maximum correlation coefficient values for 47 time intervals with at least a hundred 5-min values with the southward IMF.

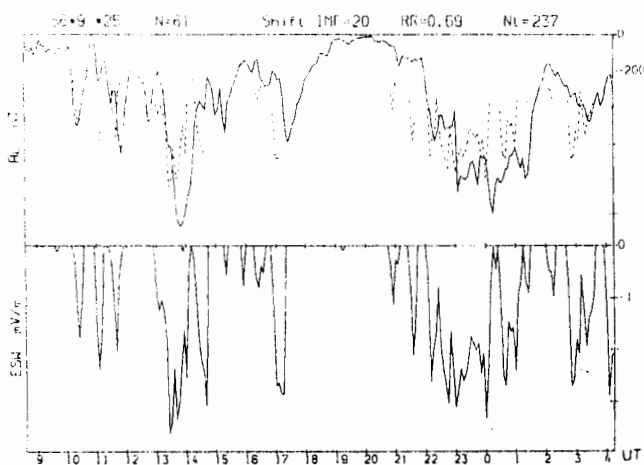


Figure 8. Example of observed (solid line) and calculated (dashed line) AL on September 25-26, 1986 for intervals with $V \cdot B_z < 0$. The time shift of 20 min was used between AL and $V \cdot B_z$ corresponding to maximum value of $RR = 0.69$. Amount of 5-min intervals $N = 237$. For 5-min intervals with $B_z > 0$ values $V \cdot B_z$ are set equal to zero.

the coupling between the solar wind and geomagnetic disturbances.

Blanchard & McPherron (Ref. 15) apply techniques of linear prediction filtering for revealing interconnection between AL and V*Bs using 117 single substorm events. It appeared, that the westward electrojet indexed by AL is controlled by two distinct processes, both proportional to V*Bs. They found that response functions AL to V*Bs have typical delays of 23 min and 63 min and that majority of auroral zone geomagnetic activity during substorms is desirable as the product of two superimposed directly driven systems. The two directly driven systems lag the solar wind electric field with a highly variable and unpredictable delay. Thus, obtained here by another method results are consistent with conclusions of Blanchard & McPherron about prevailing contribution of directly driven process to the high-latitude magnetic disturbances generation. Strong variability of time delay between events in the solar wind and magnetosphere may lead to sharp decrease of their mutual correlation when using big data arrays in the form of long time series. In this case more full description of AL indices variations assumes usage of non-linear models. One of such models was offered by Baker et al. (Ref. 14). It turns out that it is critically important to include unloading process in the model in order to replicate the main features of geomagnetic activity. However, Prichard et al. (Ref. 16) are doubtful of possibility to infer properties of the magnetosphere's behavior from observations of the behavior of the Baker et al. model. Apparently, further study of linear and non-linear processes in the coupling between the solar wind and geomagnetic activity are necessary.

5. ACKNOWLEDGMENT

This research was supported by Russian Foundation of Basic Researches grants 96-05-66279 and 96-05-65067.

6. REFERENCES

1. Akasofy S-I 1979, Interplanetary energy flux associated with magnetosphere substorms, *Planet. Space Sci.*, 27, 425 - 431.
2. Akasofy S-I 1981, Energy coupling between the solar wind and the magnetosphere, *Space Sci. Rev.*, 28, 121 - 190.
3. Baker D N & al 1986, Magnetospheric response to the IMF: Substorms, *J. Geomagn. Geoelectr.*, 38, 1047 - 1073.
4. Baker D N & al 1984, Substorms in the magnetosphere, in *Solar-Terrestrial Physics: Present and Future*, ed. by D M Butter & K Paradopoulos, NASA Ref. Publ., 1120, 8 - 13.
5. Feldstein Y I & al 1996, Electromagnetic characteristics of the high-latitude ionosphere during the various phases of magnetic substorms, *J. Geophys. Res.*, in press.

6. Feldstein Y I & A E Levitin 1986, Solar wind control of electric field and currents in the ionosphere, *J. Geomagn. Geoelectr.*, 38, 1143 - 1182.
7. Papitashvili V O & al 1994, Electric potential patterns in the northern and southern polar regions parametrized by the interplanetary magnetic field, *J. Geophys. Res.*, 99, 13251 - 13262.
8. Kamei T & al 1991, Data Book N20, World Data Center C2 for Geomagnetism, Kyoto, Japan.
9. McPherron R L 1970, Growth phase of magnetospheric substorms, *J. Geophys. Res.*, 75, 5592 - 5599.
10. Feldstein Y I 1974, Night-time aurora and its relation to the magnetosphere, *Ann. Geophys.*, 30, 259 - 272.
11. Lindqvist P-A & G T Marklund 1990, A statistical study of high-latitude electric fields measured on the Viking satellite, *J. Geophys. Res.*, 95, 5867 - 5876.
12. Baker D N 1992, Driven and unloading aspects of magnetospheric substorms, *Proceeding of the ICS-1*, Kiruna, Sweden, ESA SP-335, 185 -191.
13. Akasofy S-I 1994, Assessing the magnetic reconnection paradigm, *EOS*, 75, 249 - 252.
14. Baker D N & al 1993, Re-examination of driven and unloading aspects of magnetospheric substorms, *Adv. Space Res.*, 13, N4, 75- 83.
15. Blanchard G T & R L McPherron 1995, Analysis of the linear response function relating AL to V*Bs for individual substorms, *J. Geophys. Res.*, 100, 19155 - 19165.
16. Prichard D & al 1995, Comment on "Substorm recurrence during steady and variable solar wind driving: evidence for a normal mode in the unloading dynamics of the magnetosphere" by A J Klimas, D N Baker, D Vassiliadis, and D A Roberts; Reply, *J. Geophys. Res.*, 100, 21995 - 22001.